

Executive Summary

Widelane Grazing Angle Carrier Phase Altimetry with GNSS Reflected Signals: exploring beyond the PRETTY mission

Reference	WL_GA-CaPA_ES
Version:	1
Prepared by:	E. Cardellach
Date:	May 2022

1 Scope of the document	2
2 Objectives of the Activity	2
2.1 Context	2
2.2 Objectives	3
3 Experimental field campaign	3
3.1 GNSS-R equipment	4
3.2 Acquired data sets	4
4 Data Processing and Analysis	5
4.1 Atmospheric Effects	6
4.2 Coherence Analysis	7
4.3 Altimetric Retrievals	7
5 Recommendations to future missions	8

1 Scope of the document

This document summarizes the activity conducted under the contract ‘Widelane Grazing Angle Carrier Phase Altimetry with GNSS Reflected Signals: exploring beyond the PRETTY mission’, an Open Channel Early Technology Development Activities Evaluation Session 2020-05, ESA C.N. 4000133252/20/NL/GLC.

2 Objectives of the Activity

2.1 Context

This activity is intended to investigate the Grazing Angle (GA) Carrier Phase Altimetry (CaPA) using signals transmitted by the Global Navigation Satellite Systems (GNSS). The CaPA technique requires that the electromagnetic signal reflects coherently rather than in a diffuse regime. The hypothesis is that GA geometries enhance the likelihood of coherence scattering. It was also hypothesized that the combination of signals at slightly different frequency bands could expand the coherence conditions (widelane techniques, WL). The CaPA is a precise technique, as it is only possible when the carrier phase can be tracked, that is, when the electromagnetic wave can be measured at a fraction of a cycle. At L-band, with cycles corresponding to ~20 cm length, this maps into a few cm delay precision. Nevertheless, the use of carrier phase delay measurements tends to be relative rather than absolute (delay variations).

2.2 Objectives

Therefore, the activity focused on the following question.

QUESTION-1	Under which range of sea state and wind conditions is it possible to acquire coherent GNSS-R reflected signals? At what range of angles of observation (elevation/incidence)?
QUESTION-2	is it possible to increase the robustness to sea surface roughness (therefore increase chances of coherent scattering) when multiple carrier frequencies are combined? At which stage of the processing chain (before, during or after code demodulation) must the frequency combinations take place? Which is the optimal widelane algorithm?
QUESTION-3	Is it possible to solve the integer ambiguity of the carrier phase to obtain unambiguous sea surface height ? Under which conditions of the surface? Under which conditions of knowledge of the GNSS transmitter and receiver positions? Under which conditions of the ionospheric and tropospheric delays?
QUESTION-4	how could this concept be translated into cubesats or smallsats in Low Earth Orbiters? Are the technology requirements imposed by the concept (antenna gain and patterns, pointing and attitude control, etc) suitable for smallsats? Which coverage and spatio-temporal resolution would a future constellation provide to complement flagship radar altimetric missions? Which new science would this enable?

3 Experimental field campaign

An experimental field campaign was deployed to investigate these questions. The experiment consisted of

- **GNSS reflectometry equipment** installed on top of a mountain (39° 48' 27" N, 2° 47' 36" E, Puig Major, Mallorca, Spain), at ~1430 m altitude and close to the sea, in an enclosed military facility (Figure 1-left). The views over the sea covered up to 15° elevation angles. It collected data between 24-04-2021 and 13-07-2021, in 53 acquisitions of 30' to 2h each.
- **An oceanographic buoy** deployed in the observational zone and close to the Sentinel-3A track (N 39.88933, E 2.72217), to provide sea surface waves and wind (Figure 1-right).
- **Ancillary data** about the actual sea surface topography, in particular Sentinel-3 radar altimeter tracks crossing the observational area close to the oceanographic buoy, together with other sources of wind, waves and atmospheric conditions.



Figure 1: Location of the GNSS-R experiment in Puig Major, Mallorca, Spain (left) and deployment of the oceanographic buoy for wind and waves independent information (right). Puig Major is the highest mountain depicted in the photo.

3.1 GNSS-R equipment

The GNSS-R equipment was based on an IEEC's in-house receiver (BIBA-SPIR) that collected dual band (L1 & L5) signals from two limb-oriented directive antennas (RHCP & LHCP), sampled the I/Q components of the signals at 80 MHz in 4 bits per sample, and stored them in solid state disks before any further processing (Figure 2). This generated data at 320 MB/second rate, later processed using software receivers in the lab, for maximum flexibility even at low level steps of the processing chain.

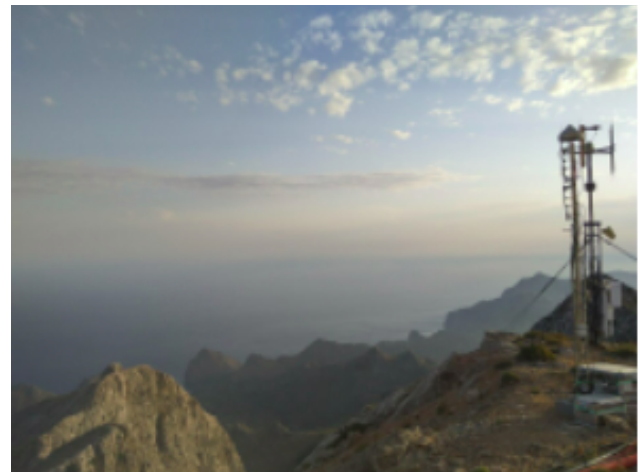
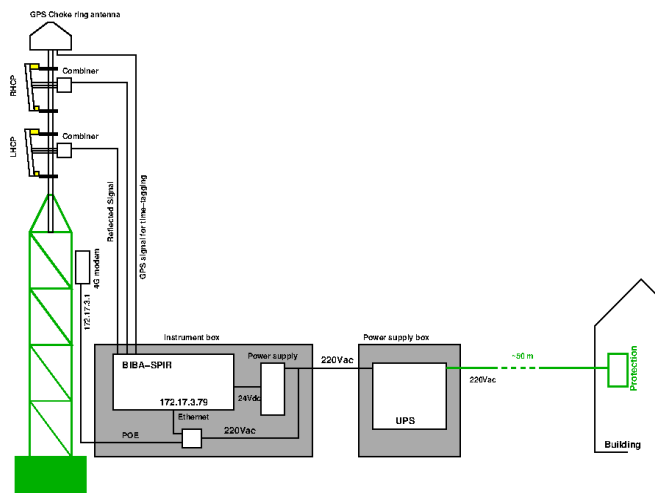


Figure 2: GNSS-R experimental set up. An sketch on the left, actual picture on the right.

The 4G connection was used to program and activate the data acquisitions. There were two incidents during the execution of the campaign: (1) replacement of the local oscillator fearing anomalous behavior; and (2) replacement of the zenith-looking antenna (for GPS time track and positioning) as it broke down. These incidents didn't have an impact on the final outcome of the campaign.

3.2 Acquired data sets

Once to twice per week, wind and waves forecasted conditions were compared to the conditions occurring during the already acquired sets. Based on this information, a new set of acquisitions was

scheduled to maximize the amount of sea surface conditions observed and guarantee co-locations when Sentinel-3 radar altimeters over-passed the region. Overall, 53 acquisitions were collected between 24-04-2021 and 13-07-2021, over sea surfaces with waves up to ~2.3 m and mean wind speeds up to ~9.5 m/s (with up to 11.5 m/s wind gusts). Each collection could contain more than one GNSS reflectometry track, from GPS, Galileo or Beidou constellations. In total, 105 GNSS-R tracks were collected, each at both frequency bands (L1 & L5) and polarizations (RH & LH) (Figure 3).

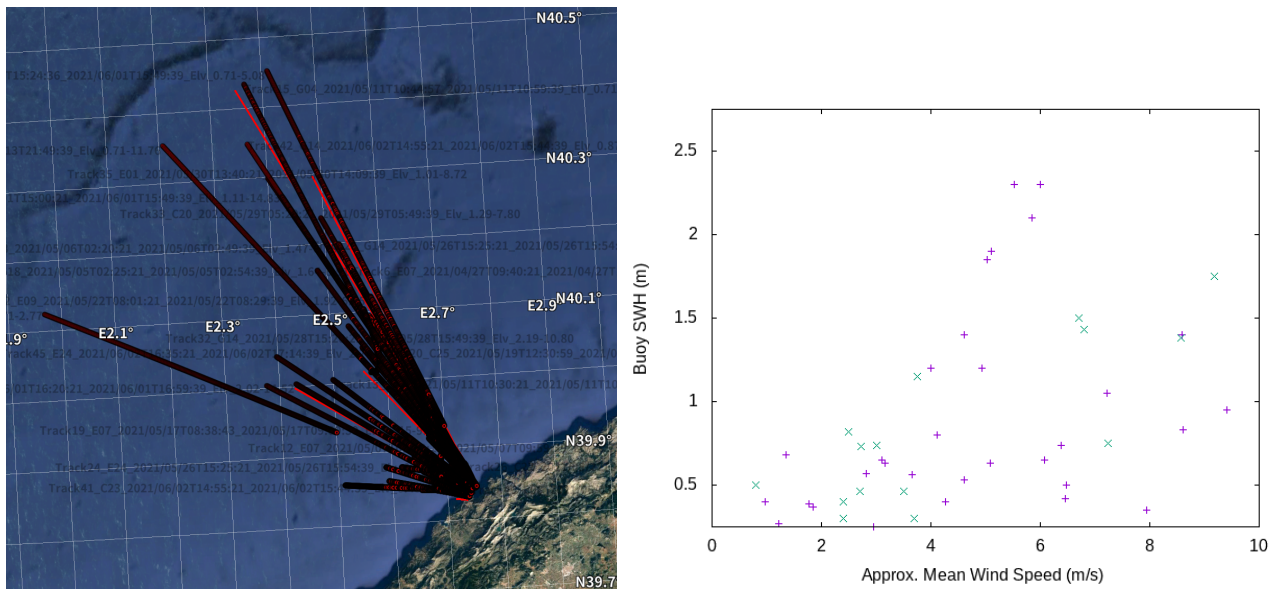


Figure 3: (left) Location of the 105 GNSS-R tracks collected during the campaign. (right) Wind and wave conditions during each of these tracks, as collected by the oceanographic buoy moored at N 39.88933, E 2.72217.

Independent information collected during the campaign includes:

- **Waves and wind:** oceanographic buoy measurements; satellite along-track observations from Sentinel-3b and Altika; satellite blended products from CFOSAT, Cryosat-2, HaiYang-2B, Jason-3, Altika, and Sentinel-3A/3B; blended multi-sensor MetOp-A/B, DMSP_F-16, DMSP_F-17 and CORIOLIS; gridded individual ASCAT scatterometers (MetOp-A/B/C); and the MedMFC and ERA-5 models.
- **Surface topography:** MedMFC forecast system, along-track radar altimeter sensors aboard Altika, H2B, Jason, Sentinel-3A/3B and Cryosat-2; daily gridded multi-satellite products; gridded CNES MSS and CLS 2015 MSS.
- **Atmospheric conditions:** ECMWF's ERA-5 for tropospheric corrections and DLR-SO's Neustrelitz Electron Density Model (NEDM) for ionospheric corrections.
- **GNSS orbits and clocks:** Multi-GNSS Experiment (MGEX) IGS products from GFZ, required for the GNSS data processing.

4 Data Processing and Analysis

The IECC software receiver was used to generate the complex waveforms for GPS, Galileo and Beidou reflected signals. This receiver works in open-loop, based on the outcome of (1) the direct signal processing and (2) geometric information of the transmitter, receiver and specular point locations and velocities (Figure 4-left). It was applied to L1/E1/B1C (1575.42 MHz), B1I (1561.098

MHz), L5/E5A/B2A (1176.45 MHz) and E5B/B2B (1207.14 MHz) signals.

Once the complex waveforms were obtained, the phase of their peak phasors was extracted and corrected for additional systematic effects such as the atmospheric induced delays, antenna offsets, and phase wind-up effects. The phases were finally unwrapped and converted to range variation measurements.

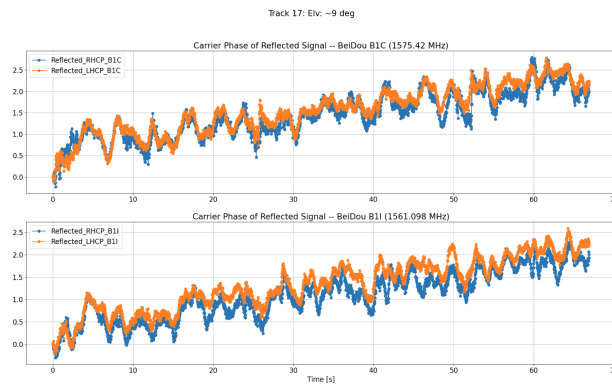
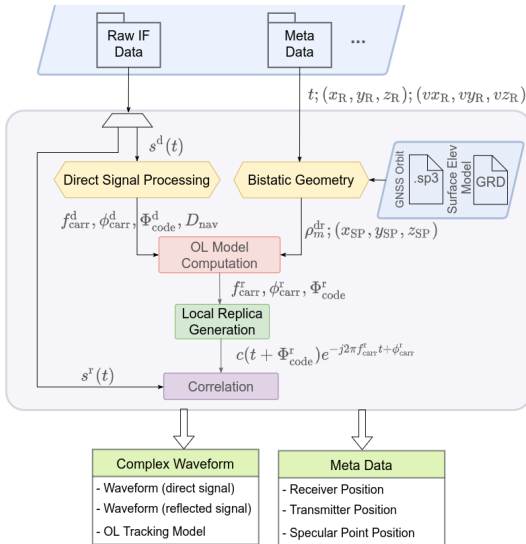


Figure 4: (left) Block diagram of the software receiver approach used to process the raw intermediate frequency data sets. (right) Example of time series of carrier phase delay for Beidou B1C and B1I signals (1575.42 MHz and 1561.098 MHz, top and bottom, respectively) at RHCP and LHCP polarizations (blue and orange, respectively).

The carrier phase delay measurements show similar fluctuations at both polarizations, but different phase variations between different frequency bands (even between B1C and B1I, only ~14 MHz apart). Experimenting with wideland frequency combinations to generate synthetic longer electromagnetic wavelengths did not expand the coherence conditions.

4.1 Atmospheric Effects

Several approaches were tested to correct the atmospheric effects: (1) mapping functions (zenithal integrated values projected down to other observational angles); (2) slant profiles (interpolation of the atmospheric variables along straight-line propagated trajectories to compute the total atmospheric induced delay); and (3) ray tracing techniques (based on 2D slices of the atmospheric conditions, the actual trajectory of the signal path is computed accounting for bending effects, to finally estimate the total delay). The mapping functions do not work properly at grazing angles of elevation; the ray tracing techniques seem accurate, but fail to converge below 3° elevation angles; while the slant profiles can extend the corrections below 3° elevation, but with suspicious jumps, especially below 1° elevation. The slant profile approach also fails to predict the re-location of the specular point due to the bending effects. The offset between the specular point location as computed along straight-lines and bended-lines can reach more than 3 km, depending on the elevation angle and the atmospheric conditions.

The processing shows that small scale features found in each frequency band cancel when using the ionospheric-free combination.

4.2 Coherence Analysis

The two main conclusions about coherence of the reflected signals are:

- Rayleigh Criterion:** the experiment confirms the Rayleigh Criterion, that can be understood as coherence holding when the full waves' volume is within the first Fresnel volume (Figure 5). If h_s is the significant wave height (approximately four time the standard deviation of the surface heights, $\sim 4 \sigma_h$), λ is the electromagnetic wavelength of the carrier frequency band, and i is the incidence angle, then coherence occurs when

$$h_s < \frac{\lambda}{2 \cos i}$$

- Widelane techniques:** we did not succeed in expanding the coherence conditions through frequency combinations.

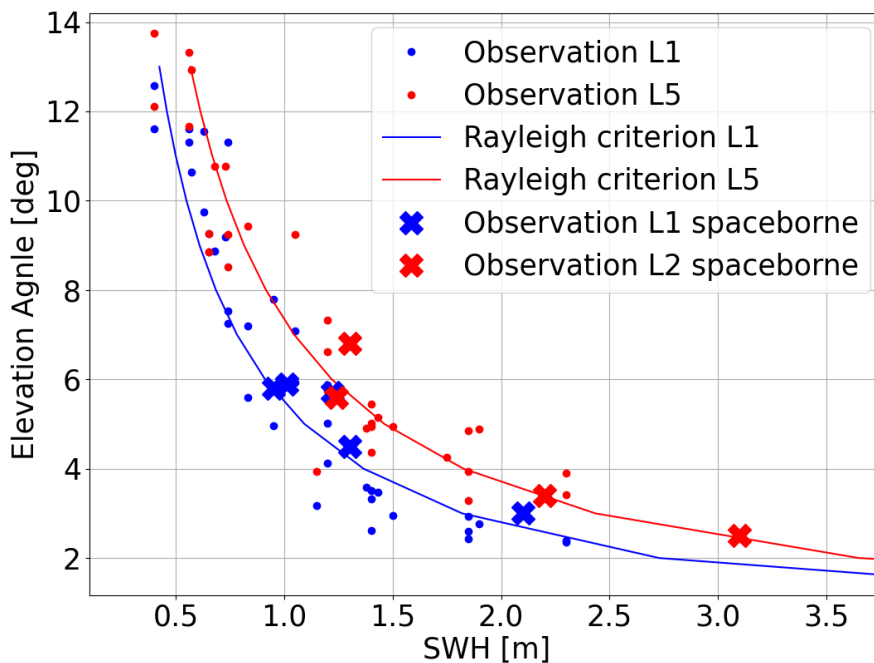


Figure 5: Elevation angle (complementary to incidence angle) at which the coherence is lost along each of the GNSS-R tracks collected in this campaign (dots), as a function of the significant wave height. Blue for L1 frequency band and red for L5. In a solid line, the Rayleigh Criterion at each frequency band. For completeness, the transitions found in spaceborne GA-CaPA events are also shown in thick crosses. They also follow the Rayleigh Criterion.

4.3 Altimetric Retrievals

The main conclusions of the altimetric retrievals are summarized below:

- Below $\sim 3^\circ$ elevation, the residual (non-corrected) systematic effects have a large impact on the solution. The current approach thus cannot be used below $\sim 3^\circ$ elevation (Figure 6-a).
- The residual phase delays present uncorrected systematic trends, most of them very similar, which seems to indicate that better modeling of all systematic effects is required (Figure 6-b). Some of the effects that have not been removed include the sea state bias, some antenna phase offsets, and second order ionospheric effects. These trends have been corrected ad-hoc.
- After the final ad-hoc corrections, the altimetric retrievals follow the surface topography, in good agreement with independent data (Figure 6-c,d).

- The precision (noise level) of the retrievals depends on the surface roughness, although always found at a few cm level.
- The accuracy (deviation from 'truth') of the retrievals is dominated by the miscorrected systematic effects. This brings the final standard deviation to values between 3 to 50 cm, with 14.2 cm mean and 10 cm median.

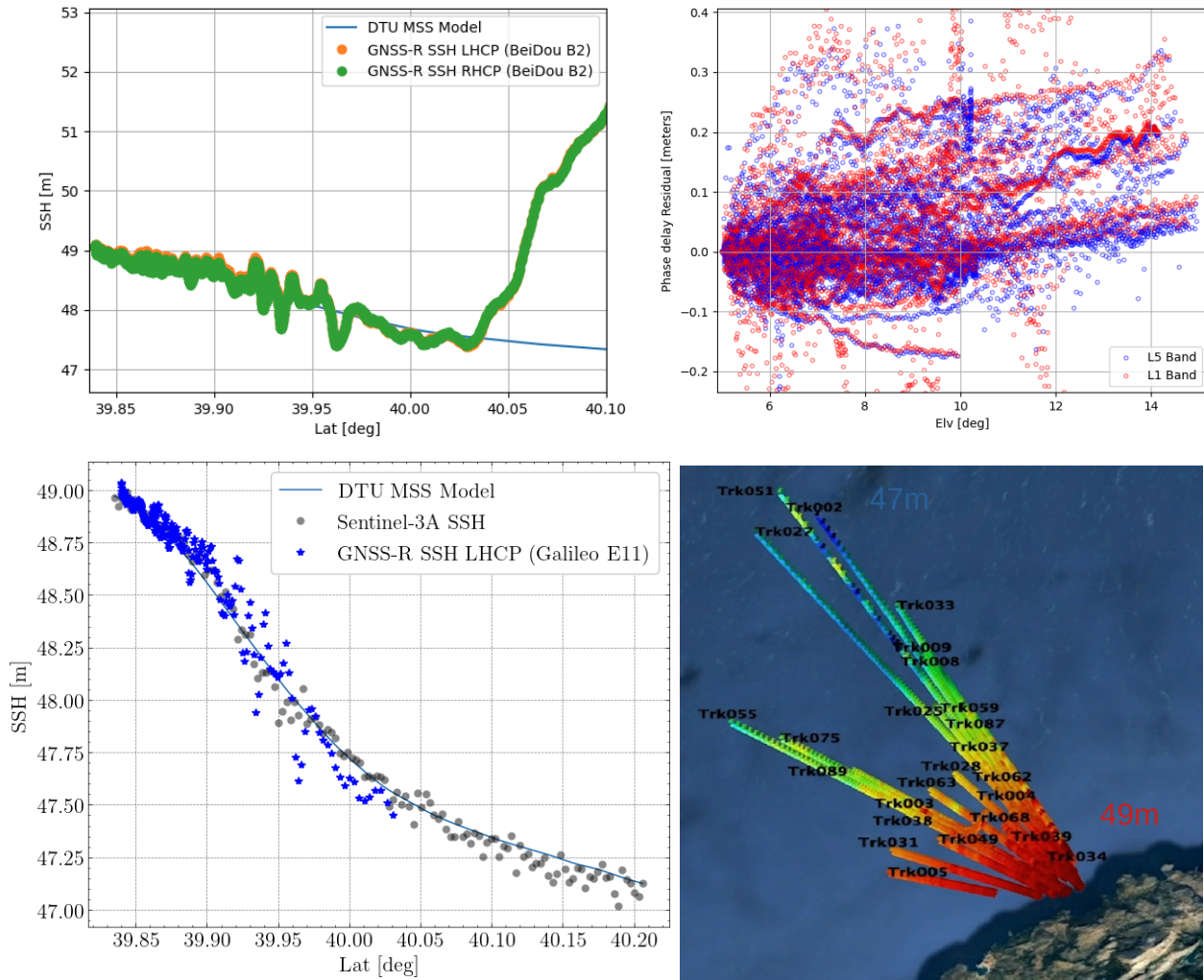


Figure 6: (a) Top-left: altimetric retrieval of one particular GNSS-R. Large errors occur below 3° elevation angles (here at latitudes above $\sim 40.3^\circ$ N). (b) Top-right: the carrier phase delays present uncorrected trends, most of them of similar slope and sign, indicating we might have consistently miscorrected one or more systematic effects. (c, d) Bottom: after an ad-hoc correction of the residual trends, the altimetric retrievals are consistent with the sea topography, as compared to Sentinel-3A (left) and within the range of mean sea surface (right, colors from 47 to 49 meter, as DTU18).

5 Recommendations to future missions

Based on these results, a set of recommendations are issued for future GA-CaPA missions:

Frequency bands	<p>To maximize the chances of coherent scattering, missions attempting GNSS-R GA-CaPA should pick frequency bands at the lower part of the GNSS spectra. Recommendation to PRETTY: use L5 instead of L1.</p> <p>Removal of residual small scale ionospheric effects requires the use of two frequency bands to synthesize the ionosphere-free combination.</p>
Signal selection	<p>These results did not identify a relationship between the performance of the carrier phase delay altimetry and their GNSS modulations. Therefore, no recommendation can be issued regarding the type of GNSS signals to be used.</p>
Antenna Orientation	<p>Antennas pointing towards the velocity and/or antivelocity of the satellite would benefit from compatibility with GNSS RO payloads.</p> <p>Side-looking antennas would benefit from longer tracks, slower evolution of elevation angle, thus longer use of the range of angles at which coherence can occur. Recommendation to PRETTY: operate with the limb-pointing antennas towards the sides of the trajectory to check the potential increase in the length of the coherent tracks. Statistical comparisons between velocity/antivelocity vs side-looking acquisitions would be advisable.</p>
Integration Time	<p>The behavior of the residual carrier phase delays below 3° elevation might indicate strong Doppler effects induced by systematic effects, thus suggesting the use of the shortest integration time possible, to avoid loss of the signal if attempting to collect signals below this threshold.</p>
Observations below 3° elevation	<p>It is recommended to study the possibility to assimilate GA-CaPA GNSS-R delay tracks down to very low elevation angles, where they are mostly coherent, into coupled atmosphere-ocean dynamics models, as a way to make the coherent very low elevation tracks useful and increase significantly the number of GNSS-R tracks with geophysical information.</p>
Geographical areas	<p>The area where the waves would enable coherence down to 5° elevation is an N-factor smaller than the area where coherence would be achieved if collecting signals down to 3° elevation. In its turn, the area where waves enable coherence by collecting signals down to 2° elevation nearly doubles the coherent area if it stops at 3°.</p>
Range of elevation angles	<p>It seems possible to correct the systematic effects (except for residual trend, to be improved) down to 3° elevation angle. The range of elevations should thus include angles down to 3°, where the chances of coherence increase. Recommendation to PRETTY: enable observations down to 3° elevation, at least in experimental mode.</p>